Supporting Information

Integration of SnO_2-MXene Photo-Supercapacitor with Perovskite Solar Cell in Two-Electrode Configuration

Ahmad Saraei[†], Ali Esfandiar*[‡†], Nima Taghavinia[†‡]

[†]Center for Nanoscience and Nanotechnology, Institute for Convergence Science and Technology (ICST), Sharif University of Technology, Tehran, Iran

[‡]Department of Physics, Sharif University of Technology, Tehran, Iran

*Email: Esfandiar@physics.sharif.edu.

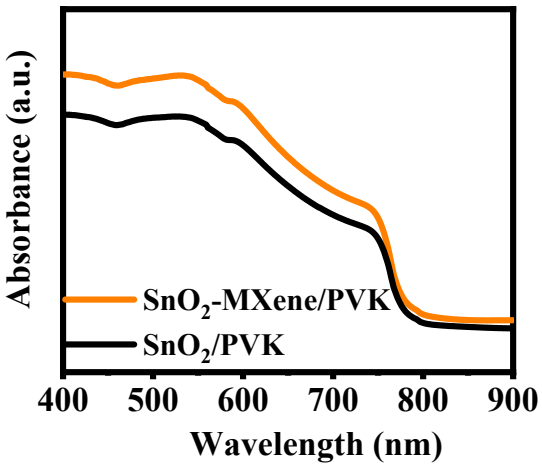

Fig. S1. UV-Vis analysis of perovskite films.

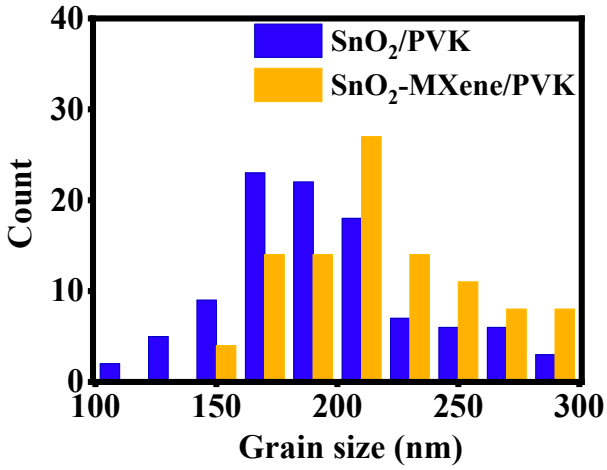

Fig. S2. The statistics of the average grain size of perovskite layers on SnO_2 and SnO_2-MXene ETLs.

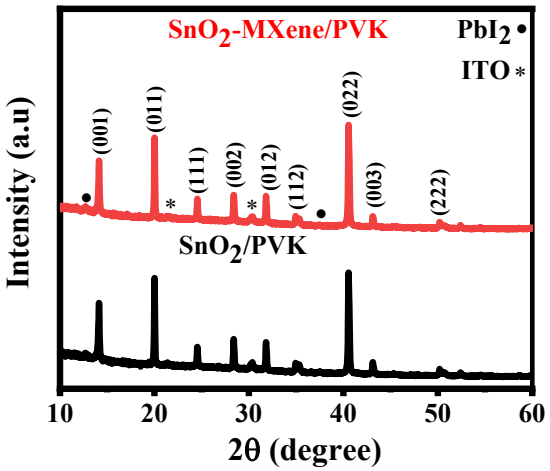

Fig. S3. XRD analysis of SnO_2/PVK and SnO_2-MXene/PVK samples.

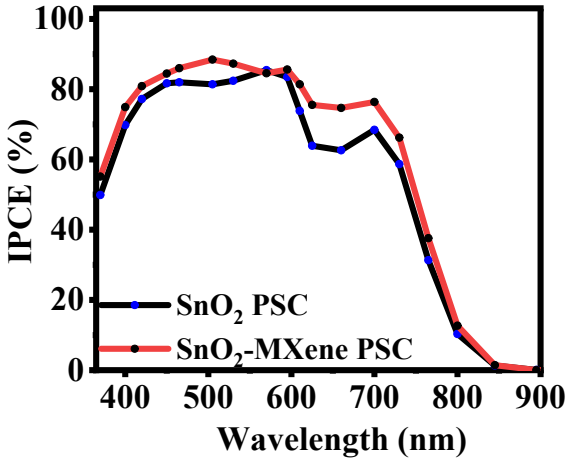

Fig. S4. The IPCE spectra performance of PSCs with SnO_2 and SnO_2-MXene ETLs.

Table S1. Equivalent circuit element values of the EIS for different PSCs.

Sample	R_1 (Ω)	R_2 (Ω)	CPE_1-T	CPE_1-P	R_4 (Ω)	L_1 (H)	R_3 (Ω)	CPE_2-T	CPE_2-P
SnO_2 PSC	4.6	730	$2e^{-8}$	0.96	3600	0.3	3182	0.00031	0.82
SnO_2-MXene PSC	3.6	665	$3e^{-8}$	0.94	2566	0.17	2900	0.0003	0.7

Table S2. Values obtained from J-V curves of best samples.

Sample	V_{oc} (V)	J_{sc} (mA/cm^2)	FF (%)	$PCE = \frac{V_{oc}.J_{sc}.FF}{P_{in}}(\%)$	R_s (Ω)	R_{sh} (kΩ)
SnO_2 PSC	0.99	19.13	56	11.20	119.8	5.2
SnO_2-MXene PSC	1.02	24.75	59	14.16	80.8	10.4

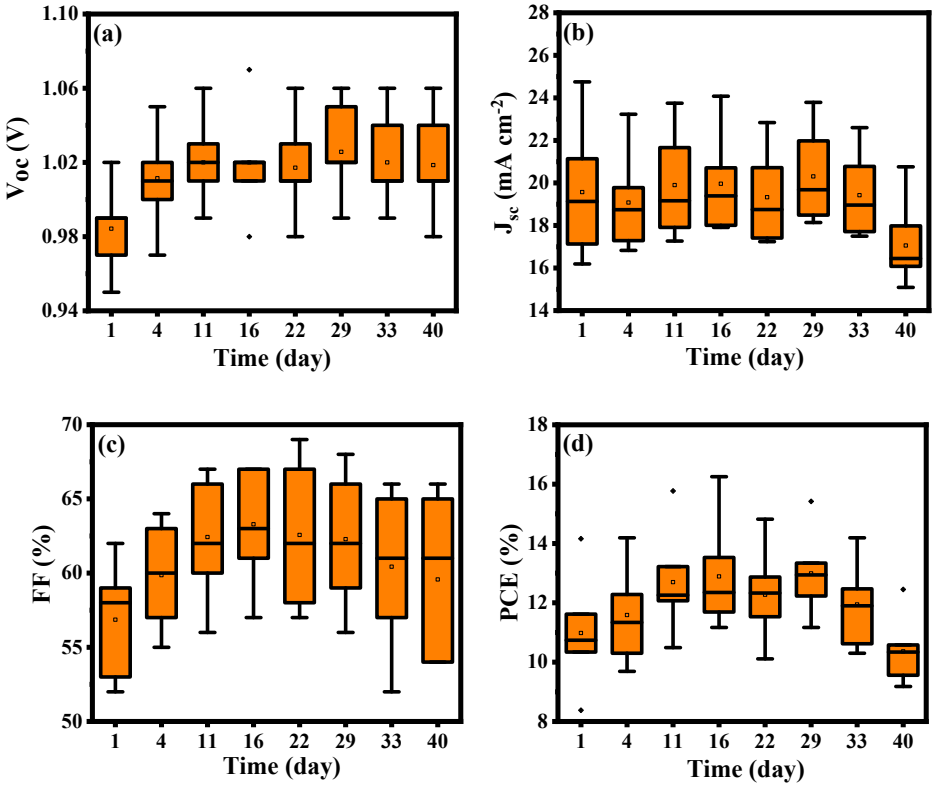

Fig. S5. Device performance statistics of (a) V_{oc}, (b) J_{sc}, (c) FF, and (d) PCE of SnO_2-MXene PSC of 10 devices.

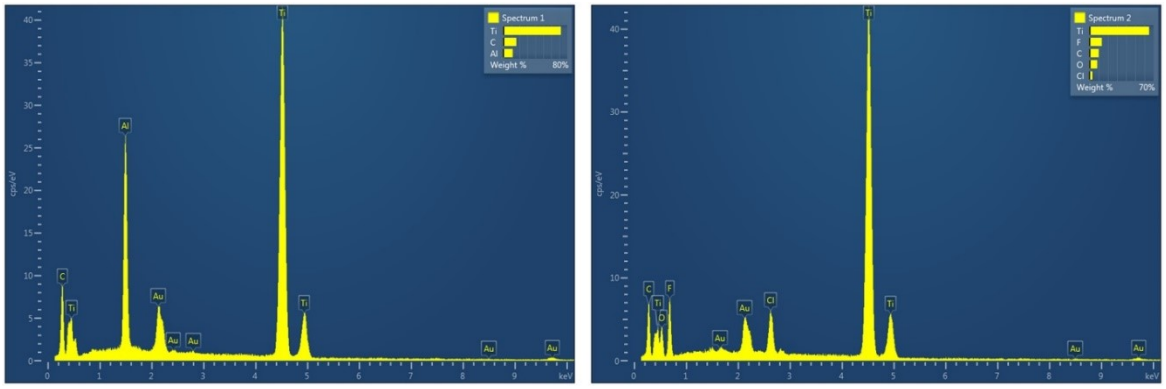

Materials	Ti (wt%)	C (wt%)	Al (wt%)	Cl (wt%)	F (wt%)	O (wt%)
MAX	72.13	16.21	11.66	0	0	0
MXene	65.15	9.97	0	3.11	13.37	8.40

Fig. S6. EDS analysis of MAX and MXene.

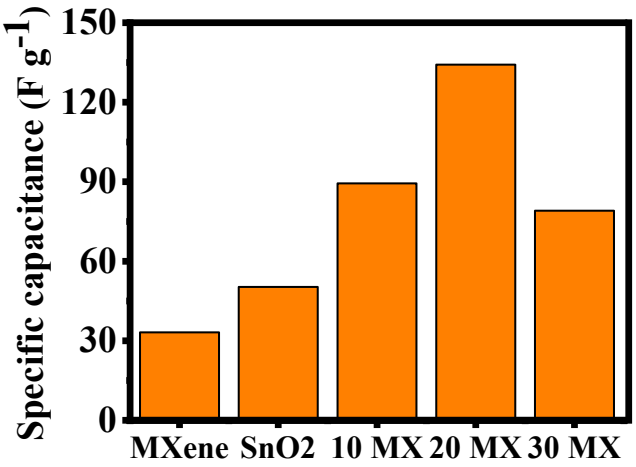

Fig. S7. Specific capacitance of the samples at a scan rate of 100 mV s^{-1}.

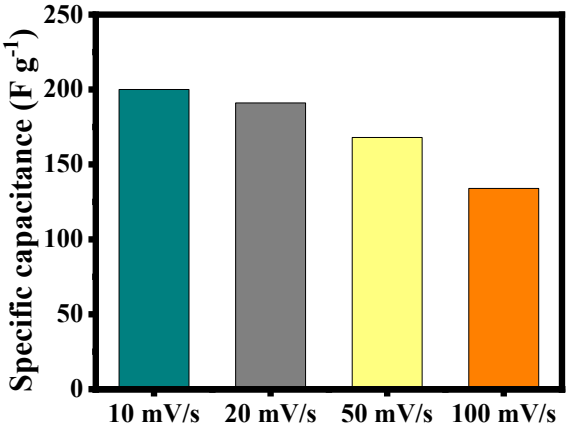

Fig. S8. Specific capacitance of 20 MX calculated at various scan rates (10–100 mV/s).

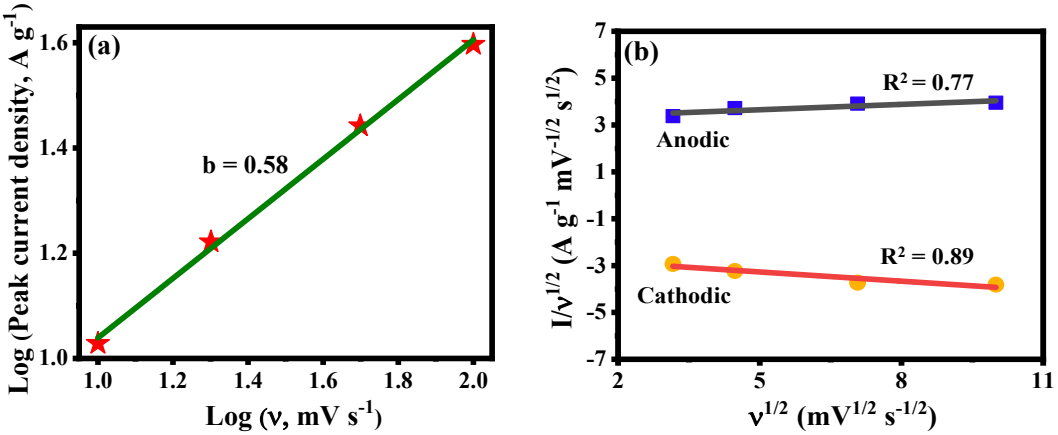

Fig. S9. (a) log-log plot of current density versus scan rate. (b) Linear fit of current density per square root of scan rate vs. square root of scan rate.

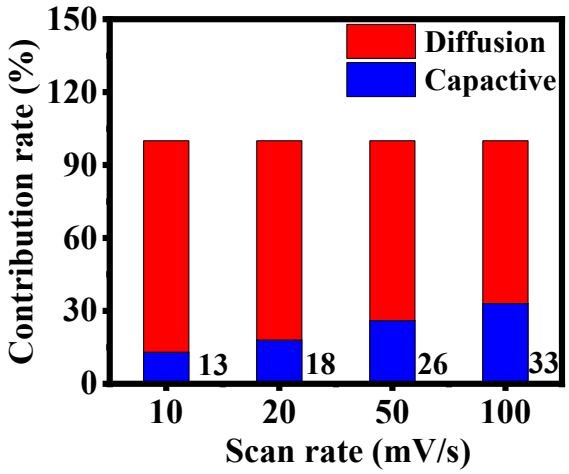

Fig. S10. Contribution ratio of 20 MX at different scan rates.

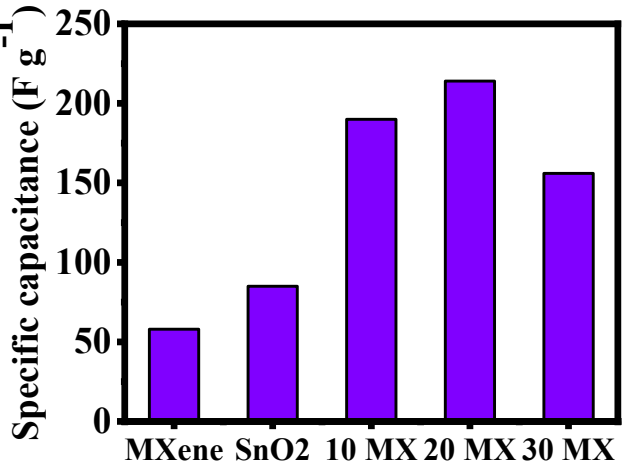

Fig. S11. The specific capacitance of SC electrodes at a current density of 2 A g^{-1}.

Sample	R_1 (Ω)	R_2 (Ω)	W_1-R	W_1-T	W_1-P	CPE-T	CPE-P
MXene	8.02	17.04	4.73	0.0031	0.416	0.0002	1.154
SnO_2	6.79	15.2	4.68	0.0042	0.429	0.0003	1.146
10 MX	3.09	9.88	4.63	0.0046	0.428	0.0004	1.091
20 MX	1.52	9.61	4.61	0.0051	0.429	0.0004	1.066
30 MX	4.53	11	4.08	0.0033	0.409	0.0002	1.149

Table S3. Equivalent circuit element values of the EIS for different SC electrodes.

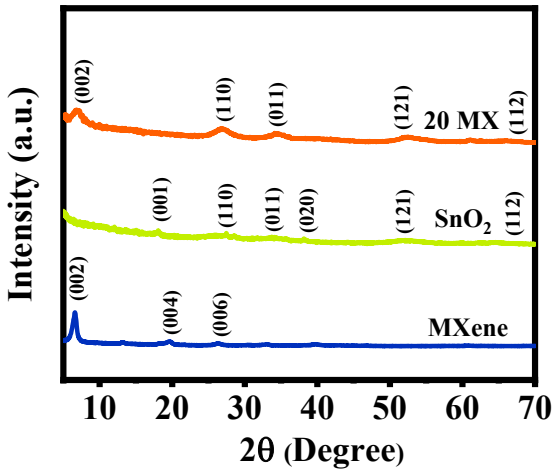

Fig. S12. XRD pattern of MXene, SnO_2, and 20 MX samples.

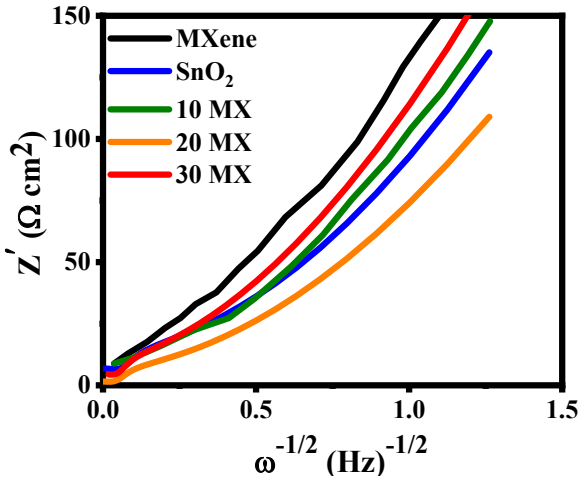

Fig. S13. Impedance (Z′) versus $\omega^{-1/2}$ plots for different SC electrodes, used to evaluate Warburg impedance and ion diffusion behavior.

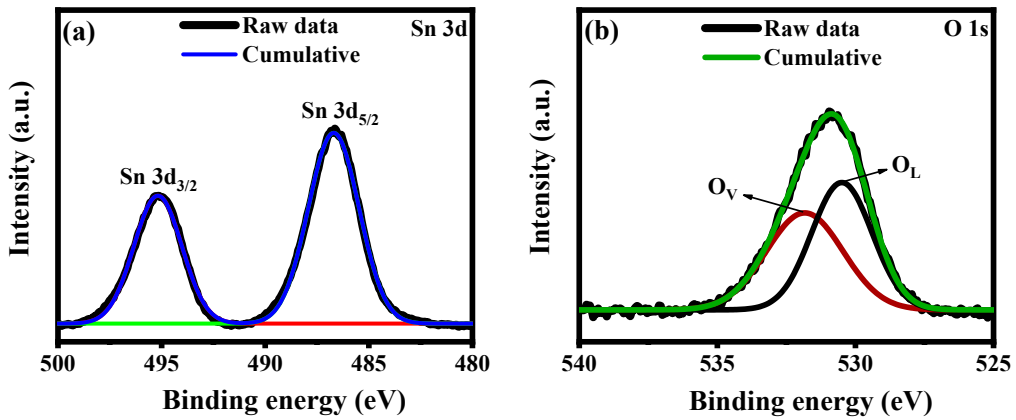

Fig. S14. High-resolution XPS spectra for SnO_2 sample (a) Sn 3d and (b) O 1s.

Table S4. Summary of monolithic integration of PSC-SC

Perovskite unit	ETL	PCE (%)	V_{oc} (V)	SC top electrode	C_{sp} or C_a of SC	Energy density of PS	year	Ref
ITO/SnO_2/$FA_{0.85}MA_{0.15}PbI_{2.55}Br_{0.45}$/CuSCN/ Carbon	SnO_2	15.54	0.97	Activated Carbon	56.75 F g^{-1} at 2 A g^{-1}	4.8 Wh kg^{-1}	2025	[1]
FTO/TiO_2/$CsPbBr_3$ /Carbon	TiO_2	5.13	1.2	Activated Carbon	–	1.1 μWh cm^{-2}	2024	[2]
ITO/PTAA/PFN/ $FA_{0.75}Cs_{0.25}Pb(I_{0.8}Br_{0.2})_3$/C60/$SnO_2$/Au	C60/ SnO_2	12.5	1.08	N-doped carbon	150 mF cm^{-2} at 0.25 mA cm^{-2}	4.2 μWh cm^{-2}	2021	[3]
Ti Foil/TiO_2 Nanotube /$Cs_{0.05}MA_{0.16}FA_{0.79}Pb(I_{0.83}Br_{0.17})_3$/PTAA/ Ag	TiO_2	13.98	1.05	Carbon	2.8 mF cm^{-2} at 100 μA cm^{-2}	0.4 μWh cm^{-2}	2022	[4]
FTO/c-TiO_2/ mp-TiO_2/$CsFA_xMA_{1-x}PbI_3$/carbon	TiO_2	14.47	0.9	$NiCo_2O_4$	404 F g^{-1} at 1 A g^{-1}	–	2020	[5]
ITO/SnO_2/TiO_2/$FA_{0.92}MA_{0.08}Pb(I_{0.92}Br_{0.08})_3$/ Spiro-OMeTAD/Au	SnO_2/TiO_2	22.44	1.17	Activated Carbon	61.9 F g^{-1} at 0.5 A g^{-1}	20.9 μWh cm^{-2}	2022	[6]
ITO/SnO_2-MXene/ $Cs_{0.05}(MA_{0.17}FA_{0.83})_{0.95}Pb(Br_{0.17}I_{0.83})_3$/CIS/Carbon	SnO_2-MXene	16.11	1.02	SnO_2-MXene	214 F g^{-1} at 2 A g^{-1}	6.8 μWh cm^{-2}	2025	**This work**

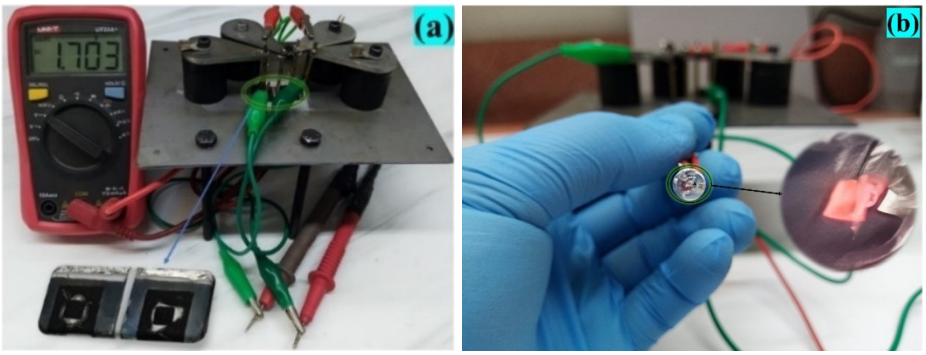

Fig. S15. Digital photograph of PS devices: (a) series-connected devices and (b) powering LED light.

1. Y. Yang, T. Yang, L. Pang, M. T. Hoang, J. Ye, C. Zhang, D. Dubal and H. Wang, Chemical Engineering Journal, 2025, 510, 161737.
2. A. Yadav, A. Saini and M. Bag, ACS Applied Materials & Interfaces, 2024, 16, 32232-32239.
3. T. Berestok, C. Diestel, N. Ortlieb, J. Buettner, J. Matthews, P. S. Schulze, J. C. Goldschmidt, S. W. Glunz and A. Fischer, Solar RRL, 2021, 5, 2100662.
4. M. Zhang and Z. Lin, ACS Energy Letters, 2022, 7, 1260-1265.
5. P. Chen, T.-T. Li, G.-R. Li and X.-P. Gao, Science China Materials, 2020, 63, 1693-1702.
6. Z. Song, J. Wu, L. Sun, T. Zhu, C. Deng, X. Wang, G. Li, Y. Du, Q. Chen and W. Sun, Nano Energy, 2022, 100, 107501.